# Micelle-based activatable probe for in vivo near-infrared optical imaging of cancer biomolecules.

AUTHOR(S):

Shimizu, Yoichi; Temma, Takashi; Hara, Isao; Makino, Akira; Yamahara, Ryo; Ozeki, Ei-Ichi; Ono, Masahiro; Saji, Hideo

CITATION:

Shimizu, Yoichi ...[et al]. Micelle-based activatable probe for in vivo near-infrared optical imaging of cancer biomolecules.. Nanomedicine : nanotechnology, biology, and medicine 2014, 10(1): 187-195

ISSUE DATE:

2014-01

URL:

http://hdl.handle.net/2433/180295

# Micelle-based Activatable Probe for *in vivo* Near-Infrared Optical Imaging of Cancer Biomolecules

Yoichi Shimizu, Ph.D.[a,b], Takashi Temma, Ph.D.[a], Isao Hara, Ph.D.[c], Akira Makino, Ph.D.[a], Ryo Yamahara, Ph.D.[c], Ei-ichi Ozeki, Ph.D.[c], Masahiro Ono, Ph.D.[a] , Hideo Saji Ph.D.[a,*]

[a] Department of Patho-Functional Bioanalysis, Graduate School of Pharmaceutical Sciences, Kyoto University, Kyoto, Japan

[b] Central Institute of Isotope Science, Hokkaido University, Sapporo, Japan

[c] Technology Research Laboratory, Shimadzu Corporation, Kyoto, Japan

**Short Title**

Activatable NIR Probe for Cancer Imaging

[*]**Corresponding Author:**

Hideo Saji, Ph.D.

Department of Patho-Functional Bioanalysis, Graduate School of Pharmaceutical

Sciences, Kyoto University, 46-29 Yoshida Shimoadachi-cho, Sakyo-ku, Kyoto 606-8501, Japan

Tel: +81-75-753-4556

Fax: +81-75-753-4568

E-mail: hsaji@pharm.kyoto-u.ac.jp

Conflict of interest: No conflict of interest

Sources of support for the research: Grants-in-Aid for Scientific Research (22791189 and 23113509) from the Ministry of Education, Culture, Sports, Science and Technology, Japan, and the New Energy and Industrial Technology Development Organization (NEDO), Japan.

149 words (Abstract)

4551 words (Complete manuscript)

42 references

5 Figures

**Abstract**

Near-infrared (NIR: 800 - 1,000 nm) fluorescent probes, which activate their fluorescence following interaction with functional biomolecules, are desirable for noninvasive and sensitive tumor diagnosis due to minimal tissue interference. Focusing on bioavailability and applicability, we developed a probe with a self-assembling polymer micelle, a lactosome, encapsulating various quantities of NIR dye (IC7-1). We also conjugated anti-HER2 single chain antibodies to the lactosome surface and examined the probe's capacity to detect HER2 in cells and *in vivo*. Micelles encapsulating 20 mol% IC7-1 (hIC7L) showed 30-fold higher fluorescence ($\lambda_{em}$: 858 nm) after micelle denaturation compared to aqueous buffer. Furthermore, antibody modification allowed specific activation of the probe (HER2-hIC7L) following internalization by HER2-positive cells, with the probe concentrating in lysosomes. HER2-hIC7L intravenously administered to mice clearly and specifically visualized HER2-positive tumors by *in vivo* optical imaging. These results indicate that HER2-hIC7L is a potential activatable NIR probe for sensitive tumor diagnosis.

**Key Words:** Lactosome; Polymeric micelle; Near-infrared Fluorescence Imaging; Activatable probe; Molecular imaging

## Background

Cancer is a major cause of death worldwide owing to vigorous cell growth, invasion, and critical metastasis induced by activation of a variety of biomolecules such as proteases [1] and growth factors [2]. Therefore, the *in vivo* detection of such biomolecules, particularly in early disease stages, is important for effective treatment with molecular target drugs [3].

Noninvasive molecular imaging techniques such as optical imaging, nuclear imaging, and magnetic resonance imaging are useful for disease detection [4]. Among these, optical imaging techniques have been widely studied and have progressed in the past decade due to their technical convenience, lack of radiation exposure, high spatial and temporal resolutions, and availability of activatable fluorescence probes [5]. To achieve highly sensitive noninvasive *in vivo* imaging with an optical imaging system, bioavailable fluorescence probes ideally would have excitation and emission wavelengths within near-infrared (NIR) region at the range of 800 - 1,000 nm, which minimizes signal attenuation and autofluorescence by tissues [6].

In our previous study, we developed a nanocarrier-based NIR probe (IC7-1 lactosome; IC7L, Fig. 1C) [7] composed of a cyanine dye ‘IC7-1’ (Fig. 1A) and an

amphiphilic polydepsipeptide (Fig. 1B). As expected, IC7L showed suitable optical characteristics for *in vivo* imaging with excitation and emission wavelengths of 830 and 858 nm, respectively [7], and could visualize tumors *in vivo* with less accumulation in the reticuloendothelial system (RES) [7-9]. However, IC7L could not distinguish tumor properties such as expression of biomolecules related to malignancy since the tumor accumulation occurred via the enhanced permeability and retention (EPR) effect.

To facilitate tumor biomolecule detection by IC7L, we sought to modify IC7L by two strategies: 1) attachment of a targeting ligand on the surface of IC7L, and 2) introduction of a signal activatable system that can suppress signals from non-targeted tissues (Fig. 1D). To make IC7L an activatable probe, we applied a self-quenching mechanism in which lipophilic dye is encapsulated at high concentrations in the hydrophobic core of the lactosome where it forms self-stacking structures that induce a quenched state. Using this strategy, we expected that the quenched probe would recognize the target-biomolecule, be delivered into the cell following biomolecule internalization, and then be dequenched to emit a fluorescence signal after probe denaturation or metabolism (Fig. 1E). As a target biomolecule, we chose human epidermal growth factor receptor 2 (HER2) due to its high expression in tumors, its close relationship with malignancy [10], and molecular its therapy applications [11]. In

addition, since HER2 is internalized after interaction with antibodies and subsequently delivered to lysosomes for degradation [12], this process can be used to trigger probe dequenching to restore fluorescence emission. Thus, HER2 is a suitable target biomolecule for both probe evaluation and future therapeutic applications.

In this study, we first prepared lactosomes encapsulating IC7-1 at a variety of concentrations, and evaluated both their quenching and dequenching properties in *in vitro* experiments. We found that lactosomes encapsulating 20 mol% IC7-1 functioned as activatable probes, and thus named this activatable probe hIC7L with “h” indicating a high dye concentration. We then conjugated an anti-HER2 single chain antibody on the hydrophilic surface of hIC7L to produce HER2-hIC7L, and evaluated its effectiveness as a targeting activatable NIR probe *in vitro* and *in vivo*. Since we also found that several other cyanine dyes could be used similarly to IC7-1 in this activatable system, we selected hCy5L (lactosome encapsulating 20 mol% Cy5) for microscopic study because the Cy5 fluorescence wavelength was preferable to IC7-1 for our microscopy experiments.

## Methods

### Preparation of IC7L

All chemicals were commercially available and of the highest purity. The amphiphilic polymer of the lactosome (Fig. 1B, polysarcosine-block-poly-L-lactate ($PSar_{70}$-block-$PLLA_{30}$) with glycol capping at the *N*-terminal) was supplied by the Shimadzu Corporation (Kyoto, Japan).

IC7L was prepared as previously described [7]. In brief, $PSar_{70}$-block-$PLLA_{30}$ (388 nmol) and IC7-1-$PLLA_{30}$ (3.9 - 97 nmol) dissolved in chloroform (500 μl) were dripped into a glass test tube. The solvent was removed under reduced pressure to form a thin film on the tube wall. Phosphate buffered saline (PBS, 0.1 M, pH 7.4) was then added to the test tube and heated at 82 ºC for 20 min. The resulting aqueous solution was filtered through a 0.20 μm Acrodisc® syringe filter (Pall Corp, East Hills, NY). The IC7L size distribution was measured at 25 ºC using a Zetasizer Nano-S90 (Malvern Instruments Ltd., UK).

IC7L (1 mg/ml, 100 μl) with an IC7-1 concentration of 1-20 mol% was incubated in 100 μl PBS (0.1 M, pH 7.4) with or without sodium dodecyl sulfate (SDS, 5% final concentration) for 30 min at room temperature. After incubation, 2.8 ml PBS was added to the solution and the fluorescence emission spectra were measured with a fluorescence

spectrometer (Fluorolog-3, HORIBA Jobin Yvon Inc., Kyoto, Japan) following excitation at 815 nm using a slit width of 5 nm for both excitation and emission measurements. The absorption spectra were measured using a UV-1800 (Shimadzu Corporation, Kyoto, Japan).

**Preparation of anti-HER2 single chain Fv anchored IC7L (HER2-IC7L)**

$PSar_{56}$-block-$PLLA_{30}$ without *N*-terminal capping was synthesized as we previously reported [8]. *N*-terminal uncapped $PSar_{56}$-block-$PLLA_{30}$ (100 mg), N-succinimidyl 3-maleimidopropionate (39.1 mg) and diisopropylethylamine (3.8 mg) were dissolved in 1.5 ml dry DMF and stirred for 7 hr at room temperature. The mixture was then purified on a size exclusion column (Sephadex LH-20, GE Healthcare, U.K.) using DMF as the eluent. The high molecular mass fraction was collected and dried *in vacuo*. Maleimide-PSar-block-PLLA (92mg, 90%); $^1$H NMR (DMSO-$d_6$) δ7.01(d, 2H, J=11.6), 5.19(t, 30H, J=7.0), 4.26-3.99(m, 150H), 2.91-2.72(m, 275H), 2.05(s, 3H), 1.46(d, 91H, J=6.8).

The maleimide-PSar-block-PLLA (194 nmol), $PSar_{70}$-block-$PLLA_{30}$ (194 nmol), and IC7-1-$PLLA_{30}$ (3.9 nmol for IC7L or 97 nmol for hIC7L) were used to prepare maleimide-IC7L/hIC7L as described above.

Anti-HER2 single chain Fv (scFv) (4D5 C10) with a cysteine at the *C*-terminus was a kind gift from CANON Inc. (Tokyo, Japan). Anti-HER2 scFv (300 μg, 100 μl PBS) was added to tris(2-carboxyethyl)phosphine hydrochloride (63.7 μg) and incubated for 2 hr on ice before purification on a size-exclusion column (Sephadex G-50, GE Healthcare, UK) to obtain the reduced form of scFv. Anti-HER2 scFv was then added to maleimide-IC7L/hIC7L (1 mg/1 ml) and incubated for 4 hr on ice with protection from light. After incubation, cysteine·HCl (158 μg) was added and further incubated for 30 min on ice. The mixture was then ultracentrifuged in an Amicon® ultra-4 Centrifugal Filter Unit (100 kDa-cutoff, Millipore, UK) to obtain HER2-IC7L/hIC7L. The purity was analyzed by size exclusion chromatography using a Superdex 200 10/300 GL column (GE Healthcare, U.K.) equilibrated with PBS at a flow rate of 0.5 ml/min. Absorbance at 215 and 830 nm was used to detect the lactosome and IC7-1, respectively, which confirmed that the absorbance peaks at both wavelengths were detected simultaneously in the high molecular weight fraction. The size distribution of HER2-IC7L was measured at 25 °C using a Zetasizer Nano-S90 and transmission electron microscopy that is described in detail in the supplementary material (Fig. S2). The concentration of anti-HER2 scFv conjugated to IC7L/hIC7L was measured by the

bicinchoninic acid (BCA) assay, and then the number (molar ratio) of the anti-HER2 scFvs per lactosome was then calculated using the estimated molecular weight values: anti-HER2, scFv, 27 kDa; IC7L, 1,172 kDa; hIC7L, 1,315 kDa. The affinity of HER2-IC7L for HER2/neu was determined by surface plasmon resonance using the ProteOn XPR36 Protein Interaction Array system (BIO-RAD Laboratories, Osaka, Japan) [13,14] with recombinant human ErbB2/HER2 Fc chimera immobilized on the sensor chip. The sensorgrams of HER2-IC7L and IC7L were fitted by a bivalent interaction model to obtain dissociation rate constants.

**Cellular uptake study**

NCI-N87 human gastric cells (ATCC, Manassas, VA, USA) (HER2-expressing tumor cells) and SUIT-2 human pancreatic carcinoma cells (Health Science Research Resources Bank, Osaka, Japan) (HER2 low-expressing cells) were cultured in RPMI1640 with 10% fetal bovine serum at 37 °C in a humidified atmosphere containing 5% $CO_2$ [15, 16]. After pre-incubation of cells ($2 \times 10^5$ cells) overnight in 24 well poly-D-lysine-coated dishes (Biocoat, Becton Dickinson), probes (40 μg/1 ml RPMI1640 with 50 μM bovine serum albumin (BSA)) were added to the cells and incubated at 37 °C in a humidified atmosphere containing 5% $CO_2$. At 1, 3 and 6 hr,

cells were washed twice with PBS and fluorescence images of the cells were acquired using a Clairvivo OPT (Shimadzu Corporation, Kyoto, Japan) with a 785 nm laser diode for excitation and a 845/55 nm bandpath filter for emission. After image acquisition, these cells were treated with 0.2 N NaOH and the cell lysate protein concentrations measured by BCA assay. The fluorescence intensity of the cells was analyzed by Clairvivo OPT display software ver. 2.60. The fluorescence intensity of the cells was represented as a ratio to the dosage as follows:

$$\text{FI ratio} = \frac{[\text{Fluorescence Intensity of the cells}]}{[\text{Fluorescence Intensity of the probe added to the cells}] \times [\text{Cell lysate(mg protein)}]}$$

For the blocking study, NCI-N87 cells ($2 \times 10^5$ cells) were treated with trastuzumab (4.7 mg/1 ml RPMI1640 with 50 μM BSA, 1000 mol-fold equivalent of HER2-IC7L) for 15 min and HER2-IC7L (40 μg) was then added. Subsequent fluorescence measurements were carried out as described above.

**Preparation of Tumor-bearing mice**

Female nude mice (BALB/c nu/nu) supplied by Japan SLC, Inc. (Hamamatsu, Japan) were housed under a 12-h light/12-h dark cycle and given free access to food and water. The animal experiments performed in this study were conducted in accordance with institutional guidelines and approved by the Kyoto University Animal Care Committee,

Japan.

NCI-N87 cells ($5 \times 10^6$ cells) suspended in 100 μl PBS containing 50 % Geltrex (Invitrogen Japan, Tokyo, Japan) were subcutaneously inoculated into the right hind legs of mice (4 week old), and an *in vivo* imaging study was performed after a 4-week growth period. In addition, for evaluation of IC7L encapsulating 20 mol% IC7-1, SUIT-2 cells ($5 \times 10^6$ cells in 100 μl PBS containing 50 % Geltrex) were also transplanted to the opposite side 2 weeks after the NCI-N87 transplantation.

**_In vivo_ imaging study**

HER2-IC7L or IC7L (2 mg / ml PBS, 100 μl) were injected into the tumor-bearing mice via the tail vein and NIR florescence images were taken using a Clairvivo OPT with a 785 nm laser diode for excitation, and a 845/55 nm bandpath filter for emission. During the imaging process, mice remained on the imaging stage under anesthesia using 2.5% isoflurane gas in oxygen (1.5 l / min). Regions of interest (ROI) were designated for the tumor and background (around the neck) on the acquired images to measure fluorescence intensities.

**Statistics**

Data are represented as the mean ± S.D. Statistical analyses were performed with two-way factorial ANOVA followed by a Tukey-Kramer test. Statistical analyses of the *in vitro* blocking study and *in vivo* study were performed with Bartlett's test followed by the Bonferroni-Holm method. A two-tailed value of $p < 0.05$ was considered to be statistically significant.

## Results

### Probe preparation and determination of optical properties

The fluorescence and absorbance spectra of IC7L with encapsulated IC7-1 concentrations varying from 1 to 20 mol% are shown in Fig. 2. The fluorescence of IC7L decreased in PBS with increasing IC7-1 concentrations used for lactosome preparation, and was similar to background levels when the IC7-1 concentration was 20 mol% (Fig. 2A). On the other hand, the IC7L fluorescence intensity increased in SDS solution as the IC7-1 concentration increased (Fig. 2B). In fact, IC7L with 20 mol% IC7-1 produced 36.1 ± 5.5 fold higher fluorescence at 848 nm in SDS solution compared to PBS, while IC7L with 1 mol% IC7-1 showed similar fluorescence intensities in both SDS solution and PBS. The absorbance spectra showed a blue-shifted band around 750 nm that increased in intensity as the IC7-1 concentration increased in PBS (Fig. 2C) and decreased in SDS solution (Fig. 2D). Based on this result, for the following study we used IC7L with 1 mol% IC7-1 as an “always-on”-type probe and IC7L with 20 mol% IC7-1 as an “activatable” type probe referred to as “hIC7L”. In addition, as shown in the supplementary material, the lactosome probes encapsulating 20 mol% of other cyanine dyes, including IR780 ($\lambda_{em}$: 812 nm), IR797 ($\lambda_{em}$: 828 nm), Cy5 ($\lambda_{em}$: 671 nm) and ICG ($\lambda_{em}$: 815 nm) also showed fluorescence activatable

properties that were similar to hIC7L (Fig.S1).

For the HER2-IC7L/hIC7L preparation, the particle sizes of HER2-IC7L, HER2-hIC7L, IC7L and hIC7L were 31.0 ± 2.7 nm (n = 3), 30.0 ± 2.5 nm (n = 6), 30.4 ± 6.0 nm (n = 3) and 30.8 ± 4.7 nm (n = 6), respectively. The estimated average molar ratio of anti-HER2-scFvs conjugated to an IC7L or an hIC7L were 5.6 ± 1.8 (n = 3) and 5.9 ± 0.9 (n = 6), respectively. The dissociation constant ($K_d$) of HER2-hIC7L against HER2 protein was about 0.014 ± 0.012 nM (n = 4). On the other hand, hIC7L did not bind to HER2 protein and a $K_d$ value could not be calculated.

**_In vitro_ study**

The uptake of probes by NCI-N87 cells (high expression levels of HER2) and SUIT-2 cells (low HER2 expression levels) was examined for 6 hr after administration (Fig. 3 and 4). With HER2-IC7L and IC7L sorted as the always-on probes (Fig. 3), the fluorescence of NCI-N87 cells at 1 hr after HER2-IC7L addition was significantly higher than that of cells treated with IC7L and eventually reached a plateau (Fig. 3A). With the activatable probes HER2-hIC7L and hIC7L (Fig. 4), HER2-hIC7L fluorescence in NCI-N87 cells increased gradually and was significantly higher than the hIC7L fluorescence in the cells 3 hr or more after addition (Fig. 4A). In contrast, probe

uptake by SUIT-2 cells (Fig. 3B and 4B) was consistently low for all four probes, and treatment with excess trastuzumab blocked uptake of HER2-hIC7L by NCI-N87 cells to levels that were similar to hIC7L uptake (Fig. 4C). Similar results were obtained with BT-474 and MCF-7 cells, which express high and low levels of HER2, respectively (Fig. S5).

The intracellular probe localization was evaluated by fluorescence microscopy using HER2-hCy5L (Cy5 was encapsulated in lactosomes instead of IC7-1), which showed that the fluorescence localization was similar to the distribution of Lysotracker (Fig. S4).

**_In vivo_ imaging study**

With the always-on probes, both HER2-IC7L and IC7L visualized NCI-N87 tumors in xenografted mice at 12 and 24 hr post-administration (Fig. 5A). However, there was no significant difference in the images and the calculated tumor-to-background (T/B) ratios between the HER2-IC7L- and IC7L-administered groups during the study duration (Fig. 5C, 1.8 ± 0.2 vs. 1.8 ± 0.1 at 12 hr and 2.0 ± 0.1 vs. 1.9 ± 0.1 at 24 hr). As for the activatable probes, HER2-hIC7L detected the NCI-N87 tumor more clearly at 12 and 24 hr post-administration than did hIC7L (Fig. 5B). In addition, the T/B ratios of

HER2-hIC7L increased with time and provided higher values than those of hIC7L (Fig. 5D, 2.4 ± 0.2 vs. 1.8 ± 0.2 at 12 hr and 2.8 ± 0.2 vs. 2.0 ± 0.3 at 24 hr). Meanwhile, the T/B ratios in the SUIT-2 tumors were unchanged regardless of the probe used (Fig. 5D, 2.0 ± 0.2 vs. 2.0 ± 0.2 at 12 hr and 2.2 ± 0.1 vs. 2.2 ± 0.1 at 24 hr). In addition, similar *in vivo* fluorescence images were also obtained in BT-474 (HER2 high expressing cells) and MCF-7 (HER2 low expressing cells) xenografted SCID mice (Fig. S6).

## Discussion

In this study, we first showed that the IC7L fluorescence was quenched with increasing concentrations of IC7-1 encapsulated in lactosomes (Fig. 2A). In the absorbance spectra, the peak around 750 nm emerged as the concentration of IC7-1 was higher in the aqueous buffer (Fig. 2C), and indicated the formation of H-dimers [17]. Furthermore, in SDS solution, the quenched IC7L fluorescence was dequenched following lactosome degradation and subsequent release of the encapsulated dyes (Fig. 2B). Similar results were also obtained with lactosomes that encapsulated other cyanine dyes at a molar ratio of 20 mol% (Fig. S1). Therefore, this quenching would be attributable to the effective stacking of cyanine dye molecules within the hydrophobic core of the lactosome due to the probe's high lipophilicity, and these results indicate that lactosomes carrying 20 mol% of cyanine dyes can serve as activatable fluorescence probes.

We then prepared HER2-hIC7L as a HER2-specific activatable NIR probe. The particle size of this probe was similar to hIC7L. Considering the smaller size of scFv (5 nm)[18] compared with the lactosome (30 nm), the occupied volume of anti-HER2-scFv in HER2-hIC7L was very low (presumed to be only about 2.7%). Therefore, the

conjugation of anti-HER2-scFv would have minimal effects on the structural properties of hIC7L. The fluorescence of HER2-hIC7L was recovered in HER2 high expressing cells but not in cells lacking HER2, and the increases in fluorescence ratios for HER2 high expressing cells were much higher for HER2-hIC7L than HER2-IC7L. In addition, the fluorescence microscopy using HER2-hCy5L rather than HER2-hIC7L revealed that the HER2-hCy5L fluorescence was localized to the lysosomes 6 hours after treatment (Fig. S4). These *in vitro* studies thus verify the mechanism of fluorescence activation in anti-HER2 scFv-conjugated lactosomes encapsulating high concentrations of cyanine dyes in that: 1) they are targeted to HER2 expressed on the cell surface of tumors, 2) are internalized via interactions with HER2, and finally, 3) probe delivery to and denaturation in the lysosomes relieves quenching, leading to fluorescence recovery.

Targeting ligands such as antibodies have been widely used in “active targeting systems” for tumor-specific imaging and drug delivery [19, 20]. Therefore, we first performed an *in vivo* study using anti-HER2-scFv conjugated to the always-on type NIR lactosomes (HER2-IC7L) with the expectation that increased accumulation in tumors induced by active targeting of HER2 would be observed. Unfortunately, there was no difference in tumor fluorescence between HER2-IC7L and IC7L (Fig. 5A, C) and

anti-HER2 scFv could not provide beneficial effects for IC7L on HER2-expressing tumor accumulation. These results might be due to a fundamental feature of lactosomes in effective tumor delivery by an EPR effect [8, 9], as was also reported in previous works using other nanocarrier probes that showed similar diminished effectiveness of antibodies for tumor targeting [21].

In contrast, compared to hIC7L, the activatable type HER2-hIC7L clearly visualized tumors expressing high levels of HER2 (Fig. 5B, D, S6). Since an antibody used as a targeting ligand was reportedly effective for increased cellular uptake of a nanocarrier probe in tumor tissue [21], anti-HER2 scFv would also likely accelerate the cellular uptake of HER2-hIC7L via interactions with HER2. This could lead to the dequenching of HER2-hIC7L inside tumor cells and provide clearer tumor images than hIC7L, while the total levels of HER2-hIC7L and hIC7L delivered in tumors might be similar with different rates of probe accumulation in intra- and extracellular spaces in tumors.

In recent years, other groups also produced studies on micelle-based activatable probe [22] having fluorescence signals that were controlled by a self-quenching mechanism that was similar to our probe. While the probes from the previous studies could visualize tumors *in vivo* by the EPR effect, probe instability remained an unsolved

issue for *in vivo* imaging of functional molecules related to tumor malignancy (about 60% of dyes were released at 24 hr after incubation in an aqueous solution). We thus employed a strategy wherein IC7-1 conjugated to the hydrophobic polymer of the lactosome (poly-L-lactic acid; PLLA) was encapsulated to form a stable complex in the lactosome core and suppressed release from the micelle [7]. On this basis, we could achieve target-specifity *in vivo* tumor imaging.

In this study we adopted HER2 as a target biomolecule because HER2 is a representative factor in molecular-targeted breast cancer therapy [11] and participates in the signal transmission of growth factors on the cell surface followed by internalization and eventual delivery to lysosomes for degradation [23]. These qualities make HER2 suitable for evaluating fluorescence activation strategies using lactosome probes. However, this approach would not be limited to HER2, but could be applied to other biomolecular targets expressed on the tumor cell surface, such as membrane type 1 matrix metalloproteinase [24, 25], folate receptors [26], epidermal growth factor receptors [27], and transferrin receptors [28]. Therefore, these results would support that hIC7L coupled with antibodies targeting such biomolecules could be promising activatable NIR probes for specific visualization of target biomolecules expressed on tumors *in vivo*. Since optical imaging technologies have been rapidly advancing in terms of both probes and

modalities such as NIR endoscopic cameras [5] and clinical breast scanners [29] and is expected especially to provide an informative navigation aid for surgery [30], such activatable NIR probes would be clinically powerful tools for the diagnosis of cancer and other diseases.

While HER2-hIC7L could visualize HER2-expressing tumors both *in vitro* and *in vivo*, significant background fluorescence was also seen in the images due to non-specific dequenching of hIC7L, which is in agreement with the observation that quenched hIC7L was gradually dequenched after 24-hour incubation in mice plasma at 37 ºC (Fig. S3). In addition, nanocarriers with neutral or positive surface charges are known to cause non-specific cell internalization as was reported in *in vitro* studies [31, 32]. Although the zeta potential of our lactosome probes was estimated to be -5.0 mV, this might not be sufficiently negative to avoid non-specific cellular uptake in tumors, especially during the delayed phase. Therefore, the improvement of *in vivo* stability and the introduction of negative charge on the probe surface should be considered in subsequent refinement of the probes to achieve higher contrast images.

Compared with other *in vivo* imaging techniques, optical imaging can greatly

benefit from activatable probes. Although a variety of activatable optical probes have been developed [5], most have excitation and emission spectra in the visible region (400 - 700 nm) and only a few lie in the NIR region (800 - 900 nm). For the two major strategies used to control probe fluorescence, photoinduced electron transfer (PeT) and Förster resonance energy transfer (FRET), there have been difficulties in developing NIR activatable probes, which for PeT may be due to the small charge separation between the highest occupied molecular orbital and the lowest unoccupied molecular orbital [5, 33], and for FRET because of the general lack of organic structures having absorption around 900 – 1,000 nm that is required for the regulation of 800 – 900 nm fluorescence [34]. Inorganic fluorescence probes such as quantum dots [35, 36] and gold nanorods [37] have developed and shown promise in *in vivo* optical imaging; however, they still invoke concerns about heavy metal toxicity [35], though some trials have been performed that avoided this potential toxicity by coating onto the probe surface with biocompatible compounds such as polyethylene glycol [38, 39] and glutathione [40]. In contrast, our probe is bioavailable since the lactosome is composed of the biodegradable materials poly-sarcosine and poly-L-lactic acid [41, 42], and, as with previous reports using lactosomes, showed no acute or transient toxicity in treated mice in all experiments [7, 9]. Therefore, hIC7L conjugated with target-specific antibody derivatives appears to be a

safe, promising, and widely applicable probe for noninvasive *in vivo* diagnostic techniques used to detect target biomolecules.

In conclusion, we developed HER2-hIC7L that shows self-quenched fluorescence and specifically interacts with HER2 expressed on tumor cells, followed by the internalization in these cells, whereupon the fluorescence is dequenched after micelle degradation. These results indicate that a targeting ligand such as an antibody-conjugated lactosome that encapsulates high concentrations of IC7-1 would be a useful NIR probe that is applicable for use in noninvasive *in vivo* optical imaging for specific detection of target biomolecules expressed in tumors.

## References

1. Egeblad M, Werb Z. New functions for the matrix metalloproteinases in cancer progression. Nat Rev Cancer. 2002;2:161-74.

2. Mendelsohn J, Baselga J. Status of epidermal growth factor receptor antagonists in the biology and treatment of cancer. J Clin Oncol. 2003;21:2787-99.

3. Gindy ME, Prud'homme RK. Multifunctional nanoparticles for imaging, delivery and targeting in cancer therapy. Expert Opin Drug Deliv. 2009;6:865-78.

4. Weissleder R, Pittet MJ. Imaging in the era of molecular oncology. Nature. 2008;452:580-9.

5. Kobayashi H, Ogawa M, Alford R, Choyke PL, Urano Y. New strategies for fluorescent probe design in medical diagnostic imaging. Chem Rev. 2010;110:2620-40.

6. Weissleder R. A clearer vision for in vivo imaging. Nat Biotechnol. 2001;19:316-7.

7. Shimizu Y, Temma T, Hara I, Yamahara R, Ozeki E, Ono M, et al. Development of novel nanocarrier-based near-infrared optical probes for in vivo tumor imaging. J Fluoresc. 2012;22:719-27.

8. Makino A, Yamahara R, Ozeki E, Kimura S. Preparation of novel polymer assemblies, "lactosome", composed of Poly(L-lactic acid) and poly(sarcosine). Chemistry Letters. 2007;36:1220-1.

9. Makino A, Kizaka-Kondoh S, Yamahara R, Hara I, Kanzaki T, Ozeki E, et al. Near-infrared fluorescence tumor imaging using nanocarrier composed of poly(L-lactic acid)-block-poly(sarcosine) amphiphilic polydepsipeptide. Biomaterials. 2009;30:5156-60.

10. Slamon DJ, Clark GM, Wong SG, Levin WJ, Ullrich A, McGuire WL. Human breast cancer: correlation of relapse and survival with amplification of the HER-2/neu oncogene. Science. 1987;235:177-82.

11. Slamon DJ, Leyland-Jones B, Shak S, Fuchs H, Paton V, Bajamonde A, et al. Use of chemotherapy plus a monoclonal antibody against HER2 for metastatic breast cancer that overexpresses HER2. N Engl J Med. 2001;344:783-92.

12. Hendriks BS, Opresko LK, Wiley HS, Lauffenburger D. Coregulation of epidermal growth factor receptor/human epidermal growth factor receptor 2 (HER2) levels and locations: quantitative analysis of HER2 overexpression effects. Cancer Res. 2003;63:1130-7.

13. Worn A, Pluckthun A. An intrinsically stable antibody scFv fragment can tolerate the loss of both disulfide bonds and fold correctly. FEBS Lett. 1998;427:357-61.

14. Bravman T, Bronner V, Lavie K, Notcovich A, Papalia GA, Myszka DG.

Exploring "one-shot" kinetics and small molecule analysis using the ProteOn XPR36 array biosensor. Anal Biochem. 2006;358:281-8.

15. Kim JW, Kim HP, Im SA, Kang S, Hur HS, Yoon YK, et al. The growth inhibitory effect of lapatinib, a dual inhibitor of EGFR and HER2 tyrosine kinase, in gastric cancer cell lines. Cancer Lett. 2008;272:296-306.

16. Steinhauser I, Spankuch B, Strebhardt K, Langer K. Trastuzumab-modified nanoparticles: optimisation of preparation and uptake in cancer cells. Biomaterials. 2006;27:4975-83.

17. West W, Pearce S. The Dimeric State of Cyanine Dyes. J Phys Chem. 1965;69:1894-903.

18. Vigor KL, Kyrtatos PG, Minogue S, Al-Jamal KT, Kogelberg H, Tolner B, et al. Nanoparticles functionalized with recombinant single chain Fv antibody fragments (scFv) for the magnetic resonance imaging of cancer cells. Biomaterials. 2010;31:1307-15.

19. Peer D, Karp JM, Hong S, Farokhzad OC, Margalit R, Langer R. Nanocarriers as an emerging platform for cancer therapy. Nat Nanotechnol. 2007;2:751-60.

20. Sahoo SK, Labhasetwar V. Nanotech approaches to drug delivery and imaging. Drug Discov Today. 2003;8:1112-20.

21. Kirpotin DB, Drummond DC, Shao Y, Shalaby MR, Hong K, Nielsen UB, et al. Antibody targeting of long-circulating lipidic nanoparticles does not increase tumor localization but does increase internalization in animal models. Cancer Res. 2006;66:6732-40.

22. Cho H, Indig GL, Weichert J, Shin HC, Kwon GS. In vivo cancer imaging by poly(ethylene glycol)-b-poly(varepsilon-caprolactone) micelles containing a near-infrared probe. Nanomedicine. 2012;8:228-36.

23. Harari D, Yarden Y. Molecular mechanisms underlying ErbB2/HER2 action in breast cancer. Oncogene. 2000;19:6102-14.

24. Osenkowski P, Toth M, Fridman R. Processing, shedding, and endocytosis of membrane type 1-matrix metalloproteinase (MT1-MMP). J Cell Physiol. 2004;200:2-10.

25. Shimizu Y, Temma T, Sano K, Ono M, Saji H. Development of membrane type-1 matrix metalloproteinase-specific activatable fluorescent probe for malignant tumor detection. Cancer Sci. 2011;102:1897-903.

26. Leamon CP, Low PS. Delivery of macromolecules into living cells: a method that exploits folate receptor endocytosis. Proc Natl Acad Sci U S A. 1991;88:5572-6.

27. Eiblmaier M, Meyer LA, Watson MA, Fracasso PM, Pike LJ, Anderson CJ.

Correlating EGFR expression with receptor-binding properties and internalization of 64Cu-DOTA-cetuximab in 5 cervical cancer cell lines. J Nucl Med. 2008;49:1472-9.

28. Hopkins CR, Trowbridge IS. Internalization and processing of transferrin and the transferrin receptor in human carcinoma A431 cells. J Cell Biol. 1983;97:508-21.

29. Tromberg BJ, Cerussi A, Shah N, Compton M, Durkin A, Hsiang D, et al. Imaging in breast cancer: diffuse optics in breast cancer: detecting tumors in pre-menopausal women and monitoring neoadjuvant chemotherapy. Breast Cancer Res. 2005;7:279-85.

30. Polom K, Murawa D, Rho YS, Nowaczyk P, Hunerbein M, Murawa P. Current trends and emerging future of indocyanine green usage in surgery and oncology: a literature review. Cancer. 2011;117:4812-22.

31. Yamamoto Y, Nagasaki Y, Kato Y, Sugiyama Y, Kataoka K. Long-circulating poly(ethylene glycol)-poly(D,L-lactide) block copolymer micelles with modulated surface charge. J Control Release. 2001;77:27-38.

32. Xiao K, Li Y, Luo J, Lee JS, Xiao W, Gonik AM, et al. The effect of surface charge on in vivo biodistribution of PEG-oligocholic acid based micellar nanoparticles. Biomaterials. 2011;32:3435-46.

33. Koide Y, Urano Y, Hanaoka K, Terai T, Nagano T. Evolution of group 14

rhodamines as platforms for near-infrared fluorescence probes utilizing photoinduced electron transfer. ACS Chem Biol. 2011;6:600-8.

34. Luo S, Zhang E, Su Y, Cheng T, Shi C. A review of NIR dyes in cancer targeting and imaging. Biomaterials. 2011;32:7127-38.

35. Wang Y, Chen L. Quantum dots, lighting up the research and development of nanomedicine. Nanomedicine. 2011;7:385-402.

36. Derfus AM, Chan, C.W.C., Bhatia, S.N. Probing the Cytotoxicity of Semiconductor Quantum Dots. Nano Lett. 2004;4:11-8.

37. Murphy CJ, Gole AM, Stone JW, Sisco PN, Alkilany AM, Goldsmith EC, et al. Gold nanoparticles in biology: beyond toxicity to cellular imaging. Acc Chem Res. 2008;41:1721-30.

38. Papagiannaros A, Levchenko T, Hartner W, Mongayt D, Torchilin V. Quantum dots encapsulated in phospholipid micelles for imaging and quantification of tumors in the near-infrared region. Nanomedicine. 2009;5:216-24.

39. Hoshino A, Manabe N, Fujioka K, Suzuki K, Yasuhara M, Yamamoto K. Use of fluorescent quantum dot bioconjugates for cellular imaging of immune cells, cell organelle labeling, and nanomedicine: surface modification regulates biological function, including cytotoxicity. J Artif Organs. 2007;10:149-57.

40. Simpson CA, Salleng KJ, Cliffel DE, Feldheim DL. In vivo toxicity, biodistribution, and clearance of glutathione-coated gold nanoparticles. Nanomedicine. 2013;9:257-63.

41. Gupta B, Revagadea N, Hilbornb J. Poly(lactic acid) fiber: An overview Progress in Polymer Science. 2007;32:455-82.

42. Tsai G, Lane HY, Yang P, Chong MY, Lange N. Glycine transporter I inhibitor, N-methylglycine (sarcosine), added to antipsychotics for the treatment of schizophrenia. Biol Psychiatry. 2004;55:452-6.

## Figure Legends

**Figure 1**. Schematic illustration of HER2-hIC7L design and strategy. A: IC7-1 chemical structure. B: Chemical structure of the amphiphilic block polymer of the "lactosome" (PSar-PLLA). C: Schematic illustration of our previously reported probe IC7L (always-on type probe) we previously reported [7]. IC7L is a lactosome that encapsulates 1 mol% IC7-1. D: Schematic illustration of the activatable type probe, HER2-hIC7L, developed in this study. The HER2-hIC7L is a lactosome encapsulating 20 mol% IC7-1 with anti-HER2 scFv conjugated to the surface. HER2-hIC7L fluorescence is quenched due to self-quenching of IC7-1 in the hydrophobic core of the lactosome. E: Schematic explanation of the HER2-hIC7L fluorescence signal activation mechanism. Quenched HER2-hIC7L first interacts with HER2 expressed on the tumor, whereupon the probe is internalized, and then dequenched with subsequent probe denaturation.

**Figure 2.** Optical characteristics of activatable type IC7L. Fluorescence emission (A, B) and absorbance spectra (C, D) of IC7L encapsulating IC7-1 molar ratios ranging from 1 (purple), 2.5 (blue), 5 (green), 10 (orange) and 20 mol% (red) after incubation in PBS buffer (A, C) or 5% SDS solution (B, D) for 30 min.

**Figure 3.** Cellular uptake of always-on type probes. NCI-N87 cells (A) or SUIT-2 cells (B) were treated with HER2-IC7L (bold line) or IC7L (dotted line). Fluorescence intensities were acquired for 6 hr. Data are expressed as the FI Ratio (mean ± S.D.) for 3-4 samples. Comparison between the HER2-IC7L-treated and IC7L-treated groups was performed with two-way factorial ANOVA followed by a Tukey-Kramer test (*$p < 0.05$ vs. IC7L).

**Figure 4.** Cellular uptake of activatable-type probes. NCI-N87 cells (A) and SUIT-2 cells (B) were treated with HER2-hIC7L (bold line) or hIC7L (dotted line), and the fluorescence intensities were acquired for 6 hr. For an inhibition study, NCI-N87 cells were pre-treated with 4.7 mg trastuzumab for 15 min and then treated with HER2-hIC7L for 6 hr (C). Data are expressed as the FI Ratio (mean ± S.D.) for 3-4 samples. Comparisons between the HER2-hIC7L-treated and hIC7L-treated groups, and among each concentration of trastuzumab-pretreated HER2-hIC7L and hIC7L addition groups were performed with two-way factorial ANOVA followed by a Tukey-Kramer test (*$p < 0.01$ vs. hIC7L), and with Bartlett's test followed by the Bonferroni-Holm method (*$p < 0.01$ vs. non- trastuzumab-pretreatment HER2-hIC7L), respectively.

**Figure 5.** *In vivo* imaging studies. A: Fluorescence images of NCI-N87 cell xenografted mice at 0 (immediately after injection), 12, and 24 hr after administration of HER2-IC7L (upper) and IC7L (lower). The yellow arrows indicate the tumor. B: Fluorescence images of NCI-N87 (right hind leg) and SUIT-2 (left hind leg) cell xenografted mice at 0 (just after injection), 12, and 24 hr after administration of HER2-hIC7L (upper) and hIC7L (lower). The yellow and red arrows indicate the HER2 high-expressing tumor (NCI-N87) and HER2 low-expressing tumor (SUIT-2), respectively. C,D: NCI-N87 and SUIT-2 tumor-to-background (T/B) fluorescence intensity ratio obtained from the region of interest of the tumor and background (around the neck) in mice administered with HER2-IC7L (red) and IC7L (blue) (C) or HER2-hIC7L (red) and hIC7L (blue) (D). Data are expressed as the T/B ratio (mean ± S.D.). Comparison of the each group was performed with Bartlett's test followed by the Bonferroni-Holm method (*$p < 0.05$).

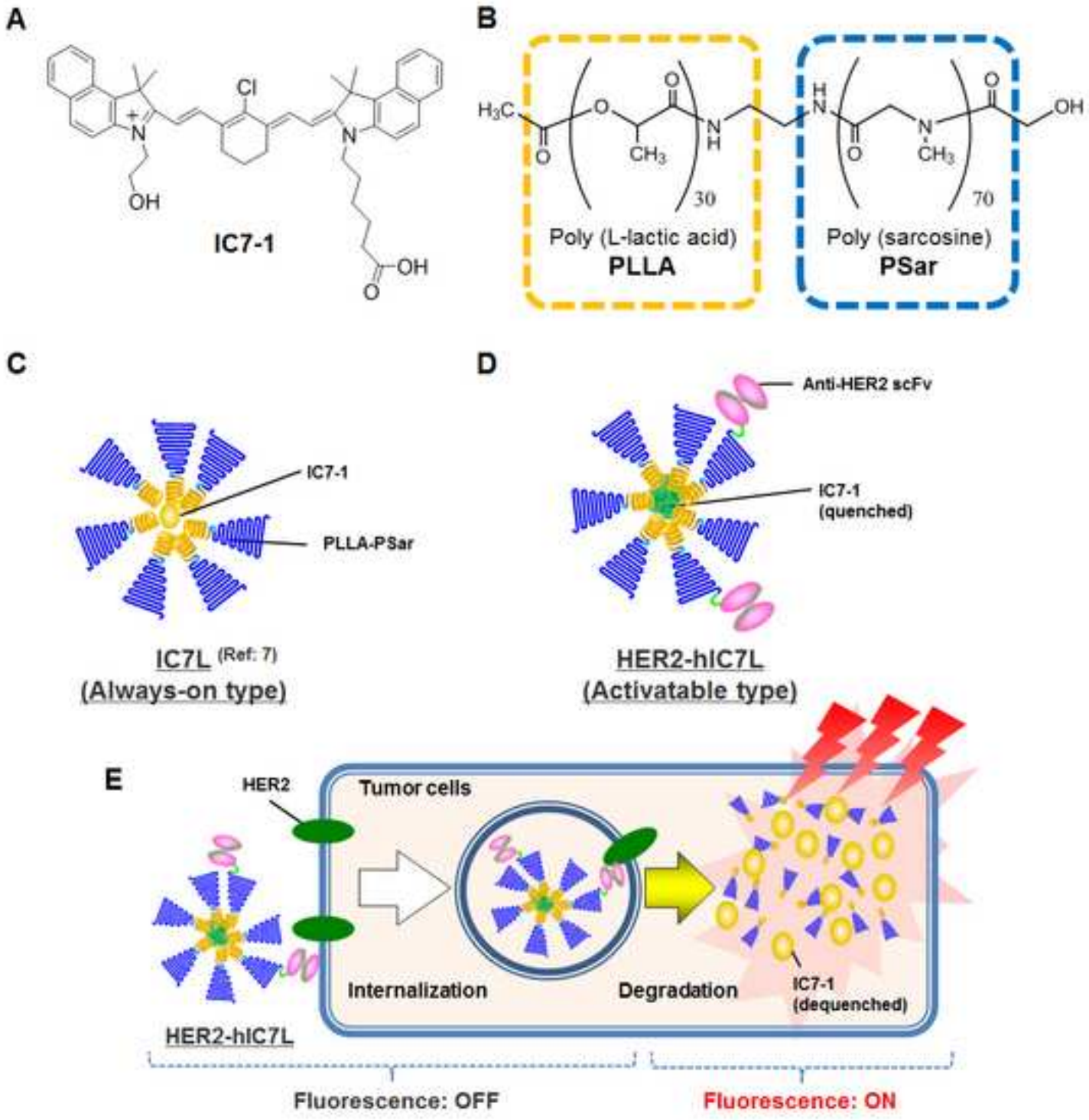

Fig 2.tif

Click here to download high resolution image

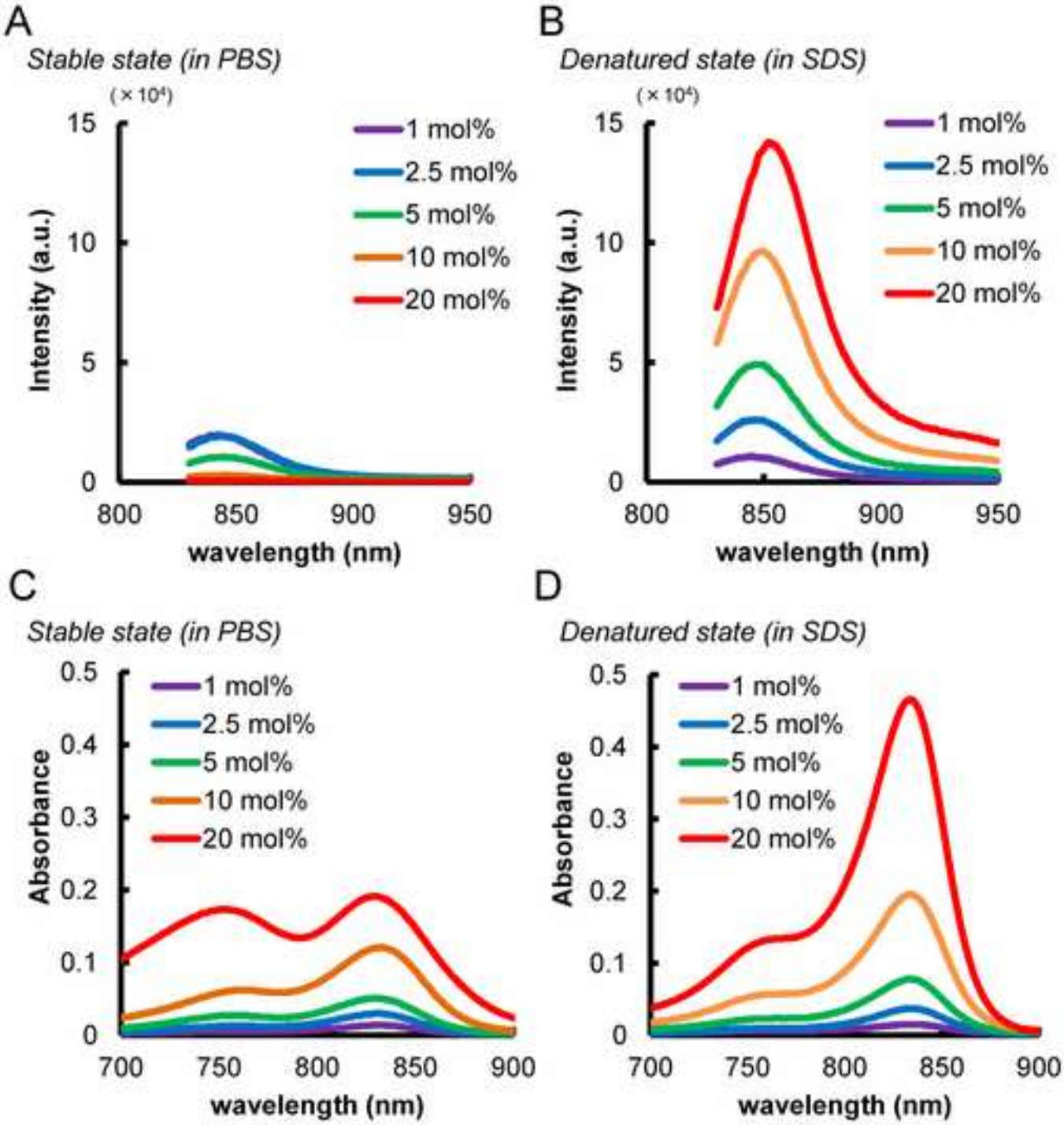

Fig 3.tif
Click here to download high resolution image

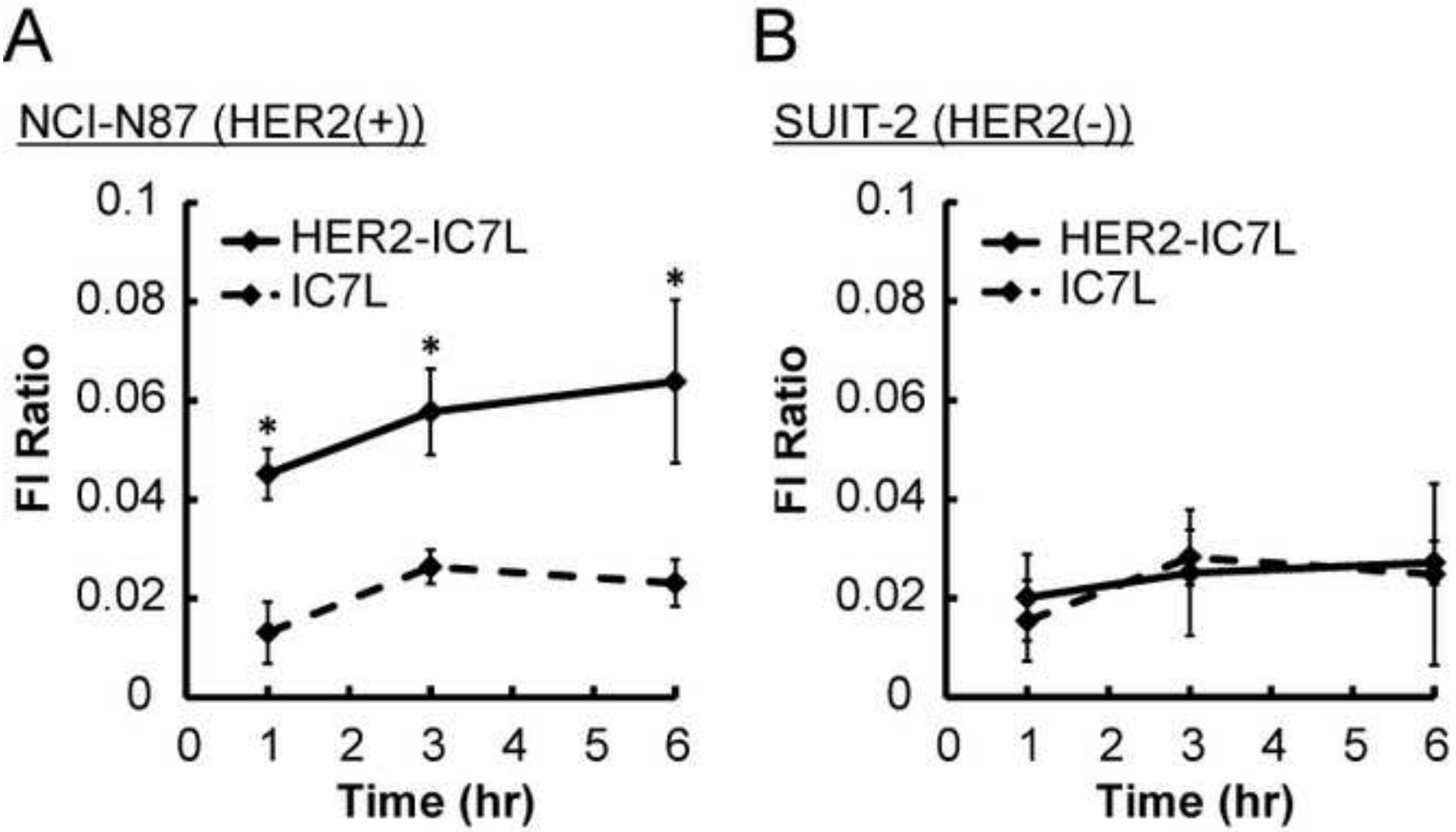

Fig 4 tif

Click here to download high resolution image

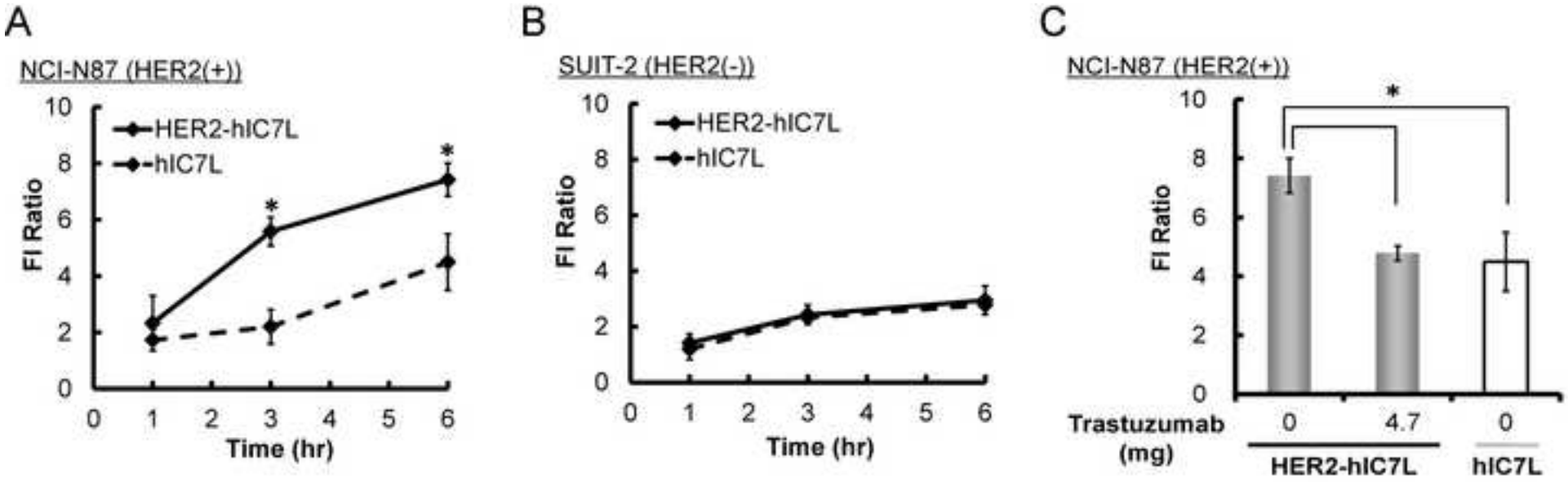

Fig 5.tif
Click here to download high resolution image